Optical model analysis of polarized neutron scattering from aluminum, copper, and chromium

G. Dagge, W. Grum, J. W. Hammer, K.-W. Hoffmann, and G. Schreder
Institut für Strahlenphysik der Universität Stuttgart, 7000 Stuttgart 80, Federal Republic of Germany
(Received 28 September 1988)

Fast neutron scattering cross section and analyzing power measurements have been performed for ^{27}Al, ^{nat}Cu, and ^{nat}Cr at incident neutron energies of $E_n = 7.62$ MeV (Al) and $E_n = 7.75$ MeV (Cu,Cr). Elastic scattering and inelastic scattering to the first excited states has been measured at angles from 21° to 124°. The scattering data obtained from the unfolded proton-recoil scintillation spectra were corrected for multiple scattering effects. Optical model parameters could be deduced by applying the excited-core weak-coupling model for a coupled channels analysis.

I. INTRODUCTION

During the last few years angular distributions of neutron differential cross section and analyzing power of nuclei covering a wide mass range have been measured at the Stuttgart SCORPION facility and analyzed by the phenomenological optical model. In the present paper experimental data of elastic and inelastic scattering at incident neutron energies of 7.75 MeV for copper and chromium and 7.62 MeV for aluminum will be compared to coupled channels (CC) optical model calculations. A 0^+-2^+ coupling basis was applied for ^{27}Al and ^{nat}Cu, while a 0^+-2^+-4^+ coupling scheme was used for ^{nat}Cr. Compound scattering processes were taken into account, if necessary.

The excited-core weak-coupling model proved to be an important tool for the investigation of odd-even nuclei. The validity of this model for aluminum and copper could be confirmed not only by cross section data but also by the corresponding analyzing power data. These data permit a more direct determination of the spin-orbit potential and furthermore, remove some of the ambiguities which would be present in cases where only cross section data were available.

II. EXPERIMENTAL PROCEDURE

A detailed description of the scattering facility SCORPION has been presented in Ref. 1. The neutrons were produced by the ^{9}Be$(\alpha,n)^{12}$C reaction with a 500 μA α beam delivered by the Dynamitron accelerator. At a reaction angle of 50° a neutron polarization of 60% was obtained. For this reaction a beryllium layer of 1.2 μm deposited on a copper backing designed for high beam powers in the kW range was used. Four NE213 scintillation counters were positioned symmetric in pairs around the scattering sample. The standard size of the sample was a 4 cm diameter by 5 cm high cylinder, which was used for Cu and Cr, while the aluminum sample was only 3 cm in diameter. The γ events could be kept below 1% by a sophisticated n-γ pulse shape discrimination.[1] A spin precession magnet allowed us to invert the direction of the spin quantization axis every 5 min in order to reduce systematical errors arising from apparative asymmetries. The background events have been determined carefully for every angular setup of the experiment, the collimators of the detectors being closed with rods of copper (15 cm) and polyethylene (60 cm), but with the sample still in position. An overall energy resolution (detectors and unfolding procedure) of about 800 keV was achieved. Additional flux monitors situated above the neutron production target as well as above, below, and behind the scattering sample provide data for a relative normalization of the scattered spectra and allow an online control of the experiment.

III. DATA EVALUATION

As a first step in data evaluation, the proton-recoil scintillation spectra were unfolded with the improved

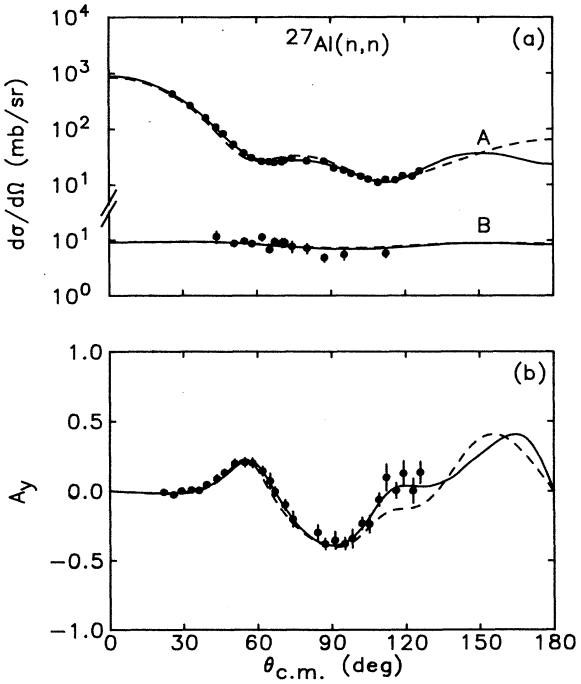

FIG. 1. Angular distributions of experimental scattering data for ^{27}Al compared to coupled channels calculations, involving a modified rotational 0^+-2^+ coupling scheme. (a) Elastic (A) and inelastic (B) differential cross section. (b) Analyzing power of elastic scattering; set Al 1 (solid); set Al 2 (dashed).

Ferdor code[2] FANTI in order to obtain the angular distributions of analyzing power and relative cross section. The relative cross section data were normalized to the $^1H(n,n)^1H$ cross section by measuring elastic scattering from a polyethylene sample.

The resulting absolute data were corrected for multiple scattering and finite geometry effects by applying the Monte Carlo code[3] XJANE, which is a modification of the well known code[4,5] JANE. This modified code provides corrections up to triple scattering sequences. For the correction of the aluminum data only single and double scattering sequences were necessary. The calculations were able to reproduce the measurements within 1% for elastic and 4% for inelastic scattering. However, the situation for copper and chromium was quite different. Since both nuclei have large total cross sections, high nuclear densities, and a large scattering cross section at forward angles, flux attenuation and multiple scattering effects for the rather large samples are high. Triple scattering sequences could not be neglected and even higher sequences had to be taken into account. Therefore, the Monte Carlo results were subjected to a last analytic correction concerning the influence of those higher scattering sequences. This method is described in detail by Ref. 6 and shall not be discussed here. Monte Carlo simulations and measurements agree within 4% for the elastic scattering data of Cu and Cr, and within 25% for the inelastic data. The final corrected experimental data are presented in Figs. 1–3. Legendre polynomial coefficients may be taken from Table I.

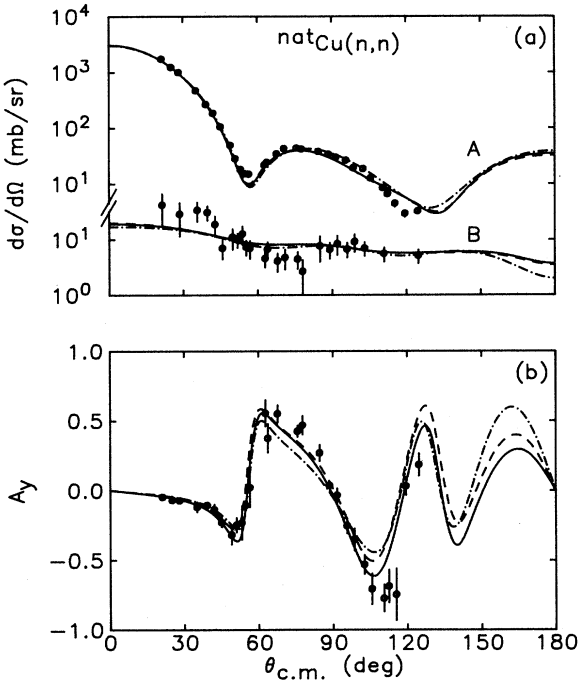

FIG. 2. Angular distributions of experimental scattering data for ^{nat}Cu compared to coupled channels calculations based on a harmonic vibrational 0^+-2^+ coupling scheme. The sum of elastic scattering and scattering from the first excited $\frac{1}{2}^-$ state is referred to as quasielastic scattering, inelastic scattering data are containing the sum of the $\frac{5}{2}^-$, $\frac{7}{2}^-$, and $\frac{3}{2}^-$ states. (a) Quasielastic (A) and inelastic (B) differential cross section. (b) Analyzing power of quasielastic scattering; set Cu 1, $W_{SO}=0.5$ MeV, $\delta_{SO}=1.5\delta_V$ (solid); set Cu 1, $W_{SO}=0.0$ MeV, $\delta_{SO}=1.0\delta_V$ (dashed); set Cu 2, $W_{SO}=0.0$ MeV, $\delta_{SO}=2.0\delta_V$ (dash-dotted).

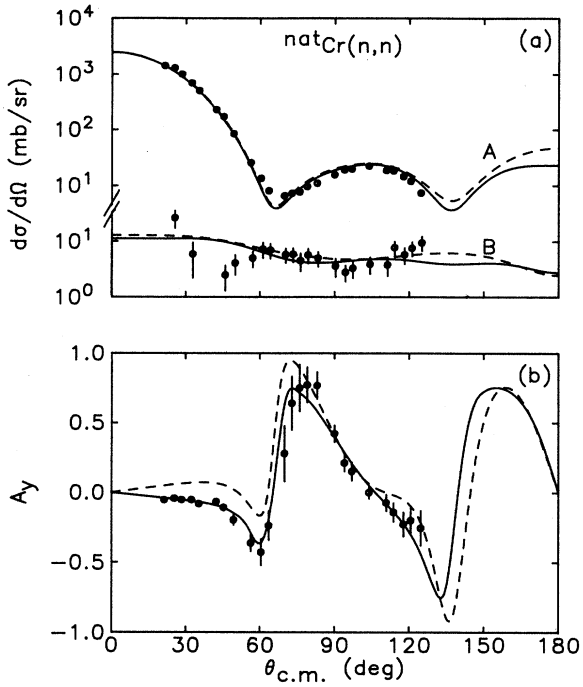

FIG. 3. Angular distributions of experimental data for ^{nat}Cr compared to coupled channels calculations based on a 0^+-2^+-4^+ anharmonic vibrational coupling scheme (set Cr 1). The dashed line shows the results for the scheme 0^+-2^+ and set Cr 2. (a) Elastic (A) and inelastic (B) differential cross section. (b) Analyzing power of elastic scattering.

IV. OPTICAL-MODEL ANALYSIS

The code[7] ECIS79 was employed to perform a coupled channels parameter search. In the present work, a deformed optical potential was used which may be expressed as follows:

$$U(r)=-Vf_V(r)+4ia_D W\frac{d}{dr}f_D(r)+\lambda\!\!\!^{-2}_{\pi}(V_{SO}+iW_{SO})\frac{1}{r}\frac{d}{dr}f_{SO}(r)(2\mathbf{l}\cdot\mathbf{s}) , \quad (1)$$

$$\lambda\!\!\!^{-}_{\pi}=\frac{\hbar}{m_\pi c}: \text{ pion Compton wavelength ;}$$

with the Woods-Saxon form factor

$$f_X(r)=\frac{1}{1+\exp\left[\frac{r-R_X}{a_X}\right]}; \quad X=V,D,\text{SO} . \quad (2)$$

TABLE I. Extracted Legendre polynomial coefficients for cross sections and analyzing powers. The differential cross section is expressed $d\sigma/d\Omega(\theta)=\sum_l a_l P_l(\cos\theta)$, while the analyzing power is expressed $A_y(d\sigma/d\Omega)=\sum_l a_l P_l^1(\cos\theta)$.

	^{27}Al		^{nat}Cu		^{nat}Cr	
	$d\sigma/d\Omega$ (mb/sr)	A_y	$d\sigma/d\Omega$ (mb/sr)	A_y	$d\sigma/d\Omega$ (mb/sr)	A_y
			Elastic scattering			
a_0	76.5	−0.98	162.1	−18.8	171.1	−6.3
a_1	133.0	0.55	384.5	15.8	341.3	−3.9
a_2	203.6	2.39	537.5	−34.0	588.5	−12.1
a_3	154.3	−0.39	544.2	11.0	464.1	−3.1
a_4	167.7	−2.12	528.5	−24.4	522.9	−5.8
a_5	78.7	−1.44	369.3	11.1	232.6	−0.3
a_6	59.0	−0.26	217.0	−8.3	212.9	−3.3
a_7	1.8	−0.17	89.4	1.6	54.3	−0.3
a_8	11.6	−0.11	28.1	−2.0	33.9	−0.9
			Inelastic scattering			
a_0	7.7	−1.1	10.7		6.4	
a_1	2.3	−0.2	8.9		3.6	
a_2	3.4	0.6	14.5		5.7	
a_3	−0.7	−0.6	9.8		7.7	
a_4			10.0		4.4	
a_5					8.3	
a_6					5.9	

The nuclear radius $R_X=r_X A^{1/3}$ can be described as an expansion in spherical harmonics for both rotational and vibrational nuclei:[8]

$$R_X=R_{0,X}\left[1+\sum_\lambda \beta_\lambda Y_\lambda^0\right]\equiv R_{0,X}+\delta R_X \ . \tag{3}$$

A deformation of the nucleus implies a coupling of the Schrödinger equations for different scattering channels. For vibrational nuclei, the Woods-Saxon form factor may be expanded in powers of δR_X, thus representing a harmonic vibrational model for an expansion to the first power of δR_X and an anharmonic model for higher powers.

A. Aluminum

Although the nucleus ^{27}Al has been subject to various investigations concerning elastic and inelastic neutron scattering cross section measurements, analyzing power data are scarce.

^{27}Al can be treated as a $2d_{5/2}$ proton hole weakly coupled to a ^{28}Si core. This excited-core model predicts a splitting of the first excited 2^+ state of ^{28}Si into a quintet of ^{27}Al as shown in Fig. 4. The inelastic cross section of the 2^+ state of ^{28}Si is divided among the levels of ^{27}Al according to their spin multiplicities.[9,10] According to the weak coupling excited-core model the inelastic cross section for a state of spin and parity J^π in ^{27}Al may be calculated from the cross section of ^{28}Si as follows

$$\frac{d\sigma}{d\Omega}(J^\pi,{}^{27}\mathrm{Al})=\frac{2J+1}{30}\frac{d\sigma}{d\Omega}(2^+,{}^{28}\mathrm{Si}) \ . \tag{4}$$

This relation has to be corrected in case that a mixing of the ground state and one of the excited states of same spin and parity occurs. For ^{27}Al this mixing of the ground state ($J^\pi=\frac{5}{2}^+$) and the second $J=\frac{5}{2}^+$ state at 2.73 MeV reduces the inelastic cross sections by a factor $(1-A^2)$ for $J^\pi\neq\frac{5}{2}^+$ and $(1-2A^2)^2$ for $J^\pi=\frac{5}{2}^+$, which is shown in Ref. 11. The mixing parameter $A^2=0.19$ was taken from Whisnant *et al.*[12] Thus, the cross section of the whole quintet is reduced to 72.5% of the 2^+ state in ^{28}Si. In order to perform a 0^+-2^+ coupled channels analysis, the reduced matrix element $\langle 0^+\|M(E2)\|2^+\rangle$ was multiplied by a factor $(0.725)^{1/2}$. A new normaliza-

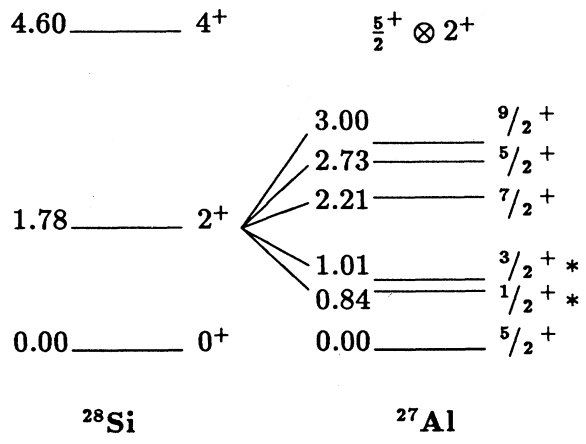

FIG. 4. The excited-core model for ^{27}Al. The 2^+ state in ^{28}Si is split into a quintet in ^{27}Al by coupling a $2d_{5/2}$ proton hole to the ^{28}Si core. An additional level at $E=2.98$ MeV not belonging to the multiplet is omitted. The observed inelastic states are marked by a *.

tion of the calculated cross section of the quintet allowed a direct comparison with the experimental inelastic data. The deformation parameters β_2 and β_4 were taken from Ref. 12, and the deformation lengths $\delta_X=\beta_X r_X$ were kept constant. An enhancement of the spin-orbit deformation length by a factor 1.2 according to Ref. 12 is possible, though not forced by the measurements.

It should be noticed that scattering data of Si and Al cannot be compared to each other in this energy region since ^{28}Si shows a strongly resonant behavior.[13] Since our measurements include only the unresolved 0.84 and 1.01 MeV states, we are not able to compare shape and magnitude of inelastic cross sections within the quintet.

Furthermore, the compound scattering cross sections are quite large. About 80% of the observed inelastic scattering cross section must be attributed to the compound nucleus (CN) process. CN contributions to the elastic scattering were remarkable, too. The CN calculations were performed with the code CERBERO,[14] taking into account the (n,n), (n,p), and (n,α) reaction channels. Optical-model (OM) parameters were taken from Ref. 12, while the Hauser-Feshbach (HF) parameters listed in Ref. 15 were used. CERBERO predicts elastic CN cross sections of about 100 mb and CN cross sections of 60 mb for the unresolved scattering to the 0.84 and 1.01 MeV states. Level width fluctuations were taken into account.

Since CERBERO results are dependent on the OM parameter set and furthermore, the calculations can only be done by a spherical optical model, the CN calculations were performed by ECIS79, too. The CN cross section is almost isotropic and influences both differential cross section and analyzing power data. Therefore, the HF parameters could be adjusted early during the first steps of the parameter search and were kept constant afterwards. CN cross sections obtained in this way were about 20% higher compared to the CERBERO results. Since the Hauser-Feshbach formula is also dependent on the spins of the states, the 0^+-2^+ coupling basis changes the shape of the CN cross section, yet this has no severe consequences in the angular range between 21° and 124°.

As can be seen in Fig. 1, the agreement between OM fits and experimental data is excellent. The corresponding OM parameters are listed in Table II (Al 1) and are compared to the results of Whisnant *et al.*[12] (Al 2), whose measurements did not include analyzing power data. Therefore, the spin-orbit parameters used by Ref. 12 are not in agreement with the CC calculations of this work. Due to the large compound cross section, the inelastic experimental data are not suited to justify the presented coupling model. Yet the excited-core model is confirmed by our elastic scattering measurements. It should be emphasized that this model is now also supported by our analyzing power measurements.

B. Copper

Both isotopes of ^{nat}Cu (68.9% ^{63}Cu, 31.1% ^{65}Cu) can be described in terms of the excited-core model, too.[16] Here a $2p_{3/2}$ proton couples to a harmonic vibrational Ni core (Fig. 5). The quartets arising from this coupling were observed, though unresolved. The scattering to the first excited states of both isotopes (0.67 MeV, 0.77 MeV) could not be separated from the elastic scattering. For further analysis, the scattering to both $\frac{5}{2}^-$ states at 1.41 and 1.62 MeV not belonging to the quartets had to be subtracted from the experimental inelastic cross section data. The ratio of cross sections from these states to the neighboring $\frac{7}{2}^-$ states was estimated to $\approx$29% for ^{63}Cu and $\approx$22% for ^{65}Cu.[17] CN processes could be neglected here.

As was stated in Refs. 17 and 18, the geometric parameters r_X and a_X are identical for both isotopes and the potential well depths do not differ much. Coupled channels calculations showed that the different mass numbers could be compensated by a change of the real well depth of about 1 MeV, which is in agreement with the results of Delaroche *et al.*[17] Thus, using the same OM parameter set and the same mass number for both isotopes should give a fairly good description of a natural copper sample. The vibrational 0^+-2^+ CC analysis performed by Delaroche *et al.* deduced different deformation parameters $\beta_2=0.22$ for ^{63}Cu and $\beta_2=0.19$ for ^{65}Cu. For these reasons our 0^+-2^+ CC analysis was performed by splitting the 2^+ level into a doublet at energies of $E(2^+,^{62}\text{Ni})=1.17$ MeV and $E(2^+,^{64}\text{Ni})=1.34$ MeV. The reduced matrix elements $\langle 0^+\|M(E2)\|2^+\rangle$ were multiplied by a factor $(0.689)^{1/2}$ and $(0.311)^{1/2}$, respectively, thus representing the mixture of both isotopes.

TABLE II. Coupled channels (CC) parameter sets for ^{27}Al, ^{nat}Cu, and ^{nat}Cr of this work compared with results from Refs. 12, 17, 19, and 21; Al 1, parameter set from this work for ^{27}Al; Al 2, parameter set from Ref. 12 for ^{27}Al (for both sets: $\beta_2=-0.36$, $\beta_4=0.20$, $\delta_{SO}=1.2\delta_V$); Cu 1, parameter set from this work for ^{nat}Cu ($W_{SO}=0.5$ MeV, $\delta_{SO}=1.5\delta_V$); Cu 2, parameter set from Refs. 17 and 19 for ^{65}Cu; Cr 1, parameter set from this work for ^{nat}Cr (0^+-2^+-4^+, second order vibrational model); Cr 2 parameter set from Ref. 21 (0^+-2^+, harmonic vibrational model).

Set	V (MeV)	r_V (fm)	a_V (fm)	W (MeV)	r_W (fm)	a_W (fm)	V_{SO} (MeV)	r_{SO} (fm)	a_{SO} (fm)
Al 1	50.7	1.19	0.67	6.75	1.31	0.50	8.8	1.17	0.46
Al 2	49.7	1.17	0.65	6.00	1.28	0.58	6.0	1.01	0.50
Cu 1	50.4	1.22	0.66	5.5	1.22	0.62	6.2	1.10	0.40
Cu 2	53.2	1.17	0.66	5.1	1.26	0.59	5.3	1.11	0.46
Cr 1	48.1	1.24	0.55	5.0	1.26	0.64	8.3	1.23	0.36
Cr 2	48.5	1.24	0.62	5.8	1.28	0.51	5.7	1.04	0.42

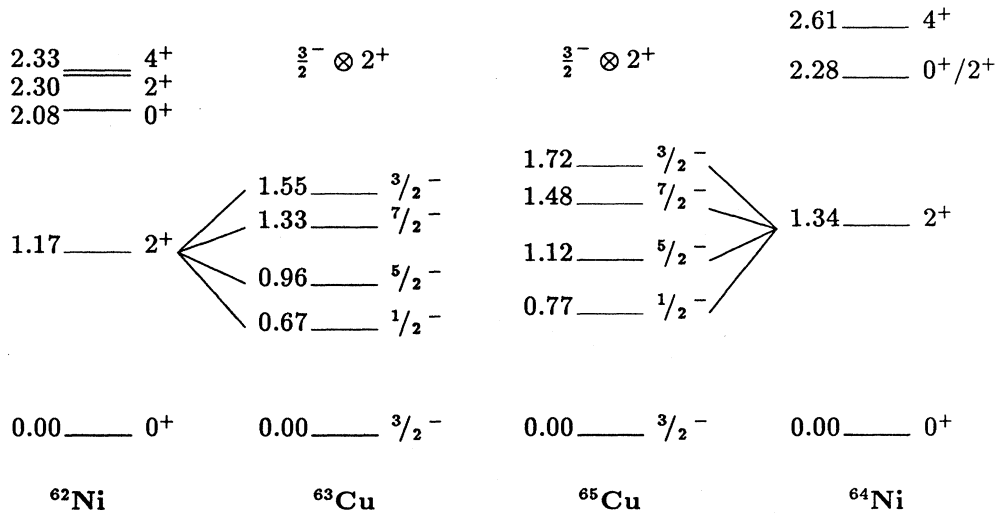

FIG. 5. The excited-core model for copper and nickel. The first excited 2^+ state of both nickel isotopes is split into a quartet for copper by coupling a $2p_{3/2}$ proton to the corresponding nickel core. For copper, the $\frac{5}{2}^-$ states not belonging to the quartets are omitted.

The results of the parameter search are presented in Fig. 2, the OM parameters are listed in Table II (Cu 1) and may be compared to the results of Refs. 17 and 19 (Cu 2). The potential well depths were calculated for 7.75 MeV from the given energy dependence. Apart from an ambiguity between V and r_V the parameters are in good agreement. The description of the data is good with the exception of the small discrepancy between measurements and OM calculations at the first minimum of the elastic differential cross section at about 55°. Measurements of Holmqvist and Wiedling[20] on natural copper are in good agreement with the data of this work. The description of the present analyzing power data confirm the results of Floyd *et al.*[19] The fits are improved by a small imaginary spin-orbit term of $W_{SO}=0.5$ MeV. Additionally, the spin-orbit deformation length was enhanced by a factor of 1.5. Since there is a strong ambiguity between these parameters, a further confinement of W_{SO} was not possible.

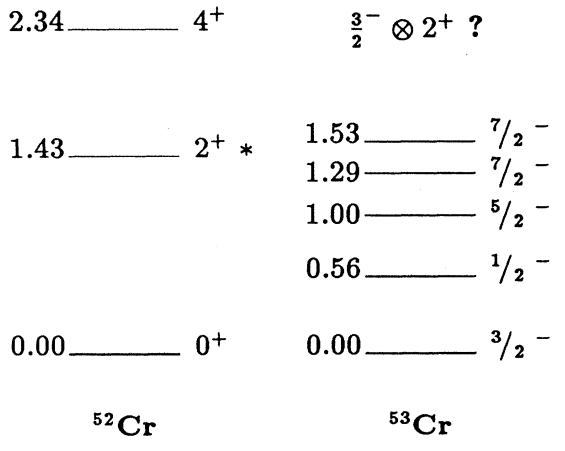

FIG. 6. Low-lying states in ^{52}Cr and ^{53}Cr. Probably the level scheme of ^{53}Cr results from coupling a $2p_{3/2}$ neutron to the ^{52}Cr core. The observed inelastic state of the main isotope is marked by a *.

C. Chromium

The main isotope of ^{nat}Cr, ^{52}Cr (83%) can be analyzed by a vibrational coupling basis. The second isotope ^{53}Cr (9.6%) can be a ^{52}Cr core coupled to a $2p_{3/2}$ neutron (see Fig. 6), thus elastic scattering of both isotopes should be quite similar to each other. Other isotopes were neglected for the analysis. Therefore, ^{nat}Cr was treated as ^{52}Cr.

The first order vibrational model based on a 0^+-2^+ coupling scheme gave a very good description of the analyzing power data but was not satisfactory for the elastic cross section measurements reported here. An imaginary spin-orbit term, a change of the deformation parameter $\beta_2=0.20$ or a coupling of further states achieved no improvements for the harmonic vibrational model.

Since the level scheme of ^{52}Cr indicates an anharmonic vibrator, an anharmonic second and third order coupling was tested. It was found that a second order vibrational 0^+-2^+-4^+ coupling basis was suited best to reproduce both cross section measurements and analyzing power data. The results of these calculations are presented in Fig. 3. A small compound cross section of about 1 mb/sr was taken into account. The corresponding OM parameters in comparison to Ref. 21 are given in Table II (Cr 1). Further improvements may be obtained by a third order model, but since the experimental data available for the calculations are not sufficient to deduce the matrix ele-

ments of the third derivative,[8] the analysis was confined to the above second order coupling basis.

V. CONCLUSION

The elastic and inelastic scattering data were well described in terms of a CC analysis applying the excited-core model for ^{27}Al, ^{nat}Cu, and ^{nat}Cr. The deduced parameters not only are in good agreement with results of other authors but also show that analyzing power data should be included for a detailed investigation. The radius parameter r_{SO} of the spin-orbit potential is in general not much smaller than the radius parameter r_V of the real part, while the spin-orbit diffuseness a_{SO} may be set to 0.4 fm. An imaginary spin-orbit potential of about 0.5 MeV was applied for ^{nat}Cu but did not improve the fits to ^{27}Al and ^{nat}Cr. The experimental cross section data from ^{nat}Cr were reproduced best by an anharmonic vibrational model, whereas the analyzing power data proved to be rather indifferent to the applied model.

ACKNOWLEDGMENTS

The authors wish to thank the accelerator staff (B. Fischer, H. Hollick, F. Kutz, and J. Lefèvre) for the provision of high beam currents for the experiment. M. Mattes (Institut für Kernenergetik und Energiesysteme Stuttgart) provided us with the most recent neutron data. We are obliged to J. Raynal [Centre d'Etudes Nucleaires (CEN) Saclay] for the provision of his code ECIS79. We would also like to thank the Gesellschaft für Elektrometallurgie, Nürnberg, for leaving us the chromium sample.

[1]J. W. Hammer, G. Bulski, W. Grum, W. Kratschmer, H. Postner, and G. Schleussner, Nucl. Instrum. Methods **244**, 455 (1986).
[2]G. Bulski, code FANTI (unpublished).
[3]W. Grum, code XJANE (unpublished).
[4]E. Woye, code JANE, private communication.
[5]E. Woye, W. Tornow, G. Mack, C. E. Floyd, P. P. Guss, K. Murphy, R. C. Byrd, S. A. Wender, R. L. Walter, T. B. Clegg, and W. Wylie, Nucl. Phys. **A394**, 139 (1983).
[6]R. C. Byrd, C. E. Floyd, K. Murphy, P. P. Guss, and R. L. Walter, Nucl. Phys. **A427**, 36 (1984).
[7]J. Raynal, coupled-channel code ECIS79 (Nuclear Energy Agency Data Bank, Gif-sur-Yvette, 1979).
[8]T. Tamura, Rev. Mod. Phys. **37**, 679 (1965).
[9]A. de-Shalit, Phys. Rev. **122**, 1530 (1961).
[10]V. K. Thankappan, Phys. Rev. **141**, 957 (1966).
[11]G. M. Crawley and G. T. Garvey, Phys. Rev. **167**, 1070 (1968).
[12]C. S. Whisnant, J. H. Dave, and C. R. Gould, Phys. Rev. C **30**, 1435 (1984).
[13]M. Koch (unpublished).
[14]F. Fabbri, G. Fratamico, and G. Reffo, code CERBERO3 (Nuclear Energy Agency Data Bank, Gif-sur-Yvette, 1977).
[15]A. Gilbert and A. G. W. Cameron, Can. J. Phys. **43**, 1446 (1965).
[16]Y. Iwasaki, G. M. Crawley, and J. E. Finck, Phys. Rev. C **23**, 1960 (1981).
[17]J. P. Delaroche, S. M. El-Kadi, P. P. Guss, C. E. Floyd, and R. L. Walter, Nucl. Phys. **A390**, 541 (1982).
[18]S. M. El-Kadi, C. E. Nelson, F. O. Purser, R. L. Walter, A. Beyerle, C. R. Gould, and L. W. Seagondollar, Nucl. Phys. **A390**, 509 (1982).
[19]C. E. Floyd, P. P. Guss, R. C. Byrd, K. Murphy, R. L. Walter, and J. P. Delaroche, Phys. Rev. C **28**, 1498 (1983).
[20]B. Holmqvist and T. Wiedling, Nucl. Phys. **A188**, 24 (1972).
[21]A. Weipert, Ph.D. dissertation, Erlangen, 1985.